# The complex X-ray morphology of NGC 7618: A major group-group merger in the local Universe?

R. P. Kraft

*Harvard/Smithsonian Center for Astrophysics, 60 Garden St., MS-67, Cambridge, MA 02138*

C. Jones

*Harvard/Smithsonian Center for Astrophysics, 60 Garden St., MS-2, Cambridge, MA 02138*

P. E. J. Nulsen

*Harvard/Smithsonian Center for Astrophysics, 60 Garden St., MS-6, Cambridge, MA 02138*

M. J. Hardcastle

*University of Hertfordshire, School of Physics, Astronomy, and Mathematics, Hatfield AL10 9AB, UK*

## ABSTRACT

We present results from a short *Chandra*/ACIS-S observation of NGC 7618, the dominant central galaxy of a nearby ($z$=0.017309, d=74.1 Mpc) group. We detect a sharp surface brightness discontinuity 14.4 kpc N of the nucleus subtending an angle of 130° with an X-ray tail extending $\sim 70$ kpc in the opposite direction. The temperature of the gas inside and outside the discontinuity is 0.79±0.03 and 0.81±0.07 keV, respectively. There is marginal evidence for a discontinuous change in the elemental abundance ($Z_{inner}$=0.65±0.25,$Z_{outer}$=0.17±0.21 at 90% confidence), suggesting that this may be an 'abundance' front. Fitting a two-temperature model to the ASCA/GIS spectrum of the NGC 7618/UGC 12491 pair shows the presence of a second, much hotter ($T=\sim2.3$ keV) component. We consider several scenarios for the origin of the edge and the tail including a radio lobe/IGM interaction, non-hydrostatic 'sloshing', equal-mass merger and collision, and ram-pressure stripping. In the last case, we consider the possibility that NGC 7618 is falling into UGC 12491, or that both groups are falling into a gas poor cluster potential. There are significant problems with the first two

models, however, and we conclude that the discontinuity and tail are most likely the result of ram pressure stripping of the NGC 7618 group as it falls into a larger dark matter potential.

*Subject headings:* galaxies: individual (NGC 7618) - X-rays: galaxies - galaxies: ISM - groups: mergers

## 1. Introduction

The complex cluster morphology seen in X-ray images and in galaxy distributions gave support to the hypothesis that large structures form hierarchically; that is, that small groups of galaxies merge to form low-mass subclusters, which then merge to form a massive rich cluster with the infalling groups aligned along large filaments. Galaxies and groups are the building blocks of the observable Universe and contain the bulk of the observable baryons. Groups are estimated to contain a significant fraction, 20-30%, of the total matter in the Universe. Thus groups are important cosmological indicators of the distribution and properties of the dark matter. However, because they are not as luminous as clusters, they have received less study than their more massive cousins.

Observations of rich clusters show many examples of pending or ongoing mergers of subclusters. In particular in X-ray cluster catalogs, about 40% of rich clusters show substructure (Jones & Forman  1984, 1999; Mohr *et al.*  1995). Virtually all stages of cluster mergers have been thoroughly investigated with both the *Chandra* and XMM-Newton observatories (Markevitch, *et al.*  2000; Vikhlinin, Markevitch, & Murray  2001; Briel, Finoguenov, & Henry  2004; Henry, Finoguenov, & Briel  2004). However, less attention has been paid to the merging of groups and the formation of low-mass clusters due to their lower X-ray luminosity and the paucity of examples in the local Universe. To our knowledge, the only nearby example of the early stages of the merger of two roughly equal mass groups is the NGC 499/NGC 507 pair (Kim & Fabbiano  1995; Kraft *et al.*  2003). In the hierarchical scenario, group mergers represent a critical transitional phase in the formation of larger scale structure. An understanding of the group merger process is thus fundamental to understanding the growth of structure.

In this paper, we report results from analysis of a short *Chandra*/ACIS-S observation of the nearby elliptical galaxy NGC 7618 ($z$=0.017309 or d$_L$=74.1 Mpc for WMAP cosmology (Spergel *et al.*  2003) - 1″=350 pc). The X-ray luminosity of NGC 7618 is $\sim$7$\times$10$^{42}$ ergs s$^{-1}$ in the 0.1-10 keV band, typical of groups, not isolated elliptical galaxies, although it appears to be optically isolated (Colbert, Mulchaey, and Zabludoff  2001). We find a sharp surface

brightness discontinuity in the X-ray emission north of of the nucleus of NGC 7618, and an extended tail to the south. We conclude that these features are either the result of a major group-group merger with UGC 12491, a group that lies 14.1′ on the sky from NGC 7618 at virtually identical redshift ($z$=0.017365) (Ebeling *et al.* 2002), or ram-pressure stripping due to infall of NGC 7618 into a larger gravitational potential (which may include UGC 12491). This pair has been poorly studied in large part because of its relatively low galactic latitude ($\ell = 105.575$, $b = -16.909$, $A_V$=0.97, $N_H$=1.19×$10^{21}$ cm$^{-2}$)).

## 2. *Chandra* and ASCA Observations

NGC 7618 was observed for 18.4 ks with Chandra/ACIS-S on December 10, 1999 (OB-SID 802). The lightcurve of events in the 5.0-10.0 keV bandpass on the entire S3 chip, excluding the NGC 7618 nucleus and any point sources visible by eye, was created using 259 s bins and examined for periods of flaring background. Intervals where the rate was more than $3\sigma$ above the mean rate were removed. There was considerable background flaring during this observations, and almost 10 ks of data were excluded. Only 8438 s of good time remained. Bad pixels, hot columns, and columns along node boundaries were also removed. We present data from the S2 and S3 chips in this paper. Absorption by foreground gas in our galaxy ($N_H$=1.19×$10^{21}$ cm$^{-2}$) was included in all spectral fits. NGC 7618 was also observed by ASCA for ∼54 ks on July 7, 1998. UGC 12491 is contained within the FOV of the ASCA/GIS, and we use these data to measure the temperature of the gas around this galaxy and the diffuse emission between NGC 7618 and UGC 12941. Data from the SIS was not used because of its smaller field of view.

## 3. Analysis

An adaptively smoothed ASCA/GIS image of the NGC 7618/UGC 12491 pair (usin the CIAO program 'csmooth') is shown in Figure 1. The optical and X-ray properties of both groups are summarized in Table 1. Their X-ray luminosities are each ∼6-7×$10^{42}$ ergs s$^{-1}$, and their X-ray emission extends to radii of 150-200 kpc. The luminosities and spatial extents far exceed those of typical isolated elliptical galaxies and are more representative of poor clusters or fossil groups (Vikhlinin, *et al.* 1999). The central elliptical galaxies represent only a small fraction of the gravitating mass that resides in a much larger dark matter halo. No optical census of the galaxy populations around either NGC 7618 or UGC 12491 has been undertaken, but their recessional velocities differ by only 17 km s$^{-1}$. The temperature of the gas around these galaxies is ∼0.8 keV, typical of groups. Based on their

X-ray luminosities, X-ray extents, and spatial proximity we conclude that these two objects are groups likely within $\sim$300 kpc of each other and gravitationally interacting.

An adaptively smoothed, exposure corrected, background subtracted *Chandra*/ACIS-S image in the 0.5-2.0 keV band of NGC 7618 is shown in Figure 2. The X-ray bright active nucleus of the host galaxy is labeled at the center. There are three unusual features to note in this image. First, the peak of the diffuse X-ray emission (shown orange in Figure 2), and therefore presumably the peak in gas density, as well as the center of the host galaxy lie $\sim$1′ North of the center of the larger scale diffuse X-ray emission (shown green). An X-ray 'tail' extends $\sim$3.3′ (69.3 kpc) South of the nucleus. The statistical significance of this 'tail' can be seen in the X-ray surface brightness profiles shown in Figure 3. These profiles were made in two 90° sectors to the North (green) and South (red) with the nucleus of NGC 7618 at the vertex. The surface brightness in the S sector at distances larger than 70″ from the nucleus is several times higher than in the North sector. Either the dark matter has a very unusual distribution, or the gas is not in hydrostatic equilibrium in the gravitational potential. Second, there is a sharp surface brightness discontinuity $\sim$41″ (14.4 kpc) North of the nucleus that spans $\sim$130°. This discontinuity is delineated by the white arrows in Figure 2. and is probably a contact discontinuity between two moving fluids. Third, on smaller scales, the X-ray emission from the gas peaks $\sim$9″ (3.2 kpc) to the E of the nucleus of the host galaxy as seen in Figure 4. In the central 10 kpc of the host galaxy, the stars will dominate the gravitating mass, so there clearly is an offset between the hot gas and the gravitating mass. All of these strongly suggest that the gas has partially separated from the gravitating matter and indicate non-hydrostatic motions.

There is an X-ray point source coincident with the optical nucleus, presumably a low-luminosity AGN. The point source contains 48 counts in the 0.5-5.0 keV band. Assuming a power-law spectrum with photon index 1.7 and galactic absorption, the X-ray luminosity of the active nucleus is $4.2\times10^{40}$ ergs s$^{-1}$ in the 0.1-10.0 keV band (unabsorbed). The X-ray luminosity of the nucleus is roughly an order of magnitude larger than that expected based on the correlation of X-ray and radio cores (Canosa, Worrall, Hardcastle, & Birkinshaw 1999). This may be a considerable underestimate if the nucleus is heavily absorbed, but is typical of that found in other "normal" elliptical galaxies (Jones *et al.* 2005).

The surface brightness profile in a 60° sector to the North of NGC 7618, shown in Figure 5, drops by approximately a factor of two across the discontinuity. At the sharpest region of the edge to the NE of the nucleus, the surface brightness drops by a factor of 4 over a distance of $\sim$4″ (1.4 kpc). The surface brightness profile in a 30° sector to the NE is shown in Figure 6. The morphology of this discontinuity is similar to that seen in *Chandra* observations of cluster 'cold-fronts', although there is no evidence for a tempera-

ture discontinuity between the two moving fluids as commonly seen in clusters of galaxies (Vikhlinin, Markevitch, & Murray 2001; Markevitch, Vikhlinin, & Mazzotta 2001; Mazzotta *et al.* 2001). We fitted absorbed APEC models to the spectra in 90° sectors of two annular regions, one inside the discontinuity and one outside. The thickness of the inner and outer annuli were $33.0''$ (11.6 kpc) and $66.4''$ (23.2 kpc), respectively. The gas temperature does not change significantly across the discontinuity ($T_{inner}$=0.785±0.025 keV, $T_{outer}$=0.810±0.070 keV). There is marginal evidence for a jump in the elemental abundance ($Z_{inner}$=0.65±0.25, $Z_{outer}$=0.17±0.21 - all uncertainties at 90% confidence), however. This suggests that the discontinuity could be an 'abundance' front due to a sharp discontinuity in the elemental abundance, and therefore the emissivity of the gas as observed in NGC 507 (Kraft *et al.* 2003). The temperature and elemental abundance structure in the gas is probably more complex than we have assumed here, but the short exposure time and limited quality of the data prevent a more detailed analysis.

Fitting power laws to the surface brightness profiles interior to and exterior to the discontinuity and assuming hydrostatic equilibrium, we find a large change in the power law index across the discontinuity, $\beta_{in}$=0.30 and $\beta_{out}$=0.64. The change in $\beta$ is almost certainly not related to a change in the gravitational potential and suggestive of non-hydrostatic gas motions. We estimate the gas density on both sides of the discontinuity by deprojecting the surface brightness profile (assuming spherical symmetry) and find proton densities of $6.0^{+1.2}_{-0.8}$ and $5.0^{+2.4}_{-1.2} \times 10^{-3}$ inside and outside the discontinuity, respectively. The upper limit of the velocity of the gas interior to the discontinuity estimated from the maximum pressure difference is Mach 0.9 or $\sim 420$ km s$^{-1}$ (Vikhlinin, Markevitch, & Murray 2001).

The X-ray morphology of the ASCA/GIS image (Figure 1) suggests that the two groups reside in a larger-scale dark matter potential. A third X-ray peak is seen $8.5'$ to the east of NGC 7618, and diffuse emission extends at least $15'$ to the north and $10'$ to the south. Any gas that resides in this larger scale dark matter halo should be hotter than the gas in the NGC 7618 group. We fitted the ASCA/GIS spectrum in three regions, two $7'$ radius circles centered on each galaxy and a third region $15'$ in radius centered between NGC 7618 and UGC 12491 excluding the two $7'$ radius circles centered on each galaxy. The radius of the two circles centered on NGC 7618 and UGC 12491 corresponds to the 90% encircled energy radius for the ASCA/GIS in the 1-2 keV band. Background was determined from ASCA/GIS high-latitude, blank sky observations taken from the HEASARC and generated using the FTOOL 'mkgisbgd'.

We fit absorbed, single temperature APEC models to each spectrum with $N_H$ frozen at the Galactic value and the elemental abundance frozen at $0.6Z_\odot$. The results of these fits are summarized in the top half of Table 2. Single temperature models are poor fits for

the regions centered on NGC 7618 and UGC 12491, but provide an adequate description of the diffuse emission between the galaxies. The temperature of the diffuse gas between NGC 7618 and UGC 12491 is $2.32^{+0.50}_{-0.34}$. We also fit two temperature models to the two spectra extracted from the regions centered on NGC 7618 and UGC 12491. As before, both the $N_H$ and the elemental abundance were frozen. For NGC 7618, we also froze the temperature of one component at 0.8 keV, the value determined from the ACIS-S spectral fitting, to reduce the number of free parameters. If this parameter is allowed to freely vary, the fit value is consistent with 0.8 keV. For UGC 12491, the temperatures of both components were allowed to freely vary. The results of these fits are summarized in the bottom half of Table 2. The two temperature model provides acceptable fits in both cases, and the temperature of the hotter component is ∼2.3 keV.

## 4. Discussion

There are at least four possible explanations for the observed X-ray structures. First, the complex X-ray morphology could be the result of a radio lobe/IGM interaction. NGC 7618 is a radio source. It is detected in the NVSS with a flux density of 20 mJy, with some evidence of extension NW/SE. At higher frequencies (5 and 8 GHz) two 15-min archival VLA observations only detect a point-like core coincident with the center of the galaxy, with a flux density of 4.5 mJy at 4.9 GHz and 3.0 mJy at 8.4 GHz. However, at lower frequencies, the flux density is much higher: 1.2 Jy in the 151-MHz 6C catalog (Hales, Baldwin, & Warner 1993), 0.26 Jy in the 408-MHz B3 catalog (Ficarra, Grueff, & Tomassetti 1985), and 1.0 Jy in the 74-MHz VLA Low-Frequency Sky Survey (VLSS: http://lwa.nrl.navy.mil/VLSS/). The high flux density at low frequencies suggests that there may be a relic radio source, the aged synchrotron plasma from a more energetic phase of the active nucleus. The X-ray morphology is very different from that seen in other examples of radio lobe/ISM interactions, however. There are no obvious X-ray cavities as are commonly seen in such radio lobe/ISM interactions (e.g. (McNamara *et al.* 2000; Jones *et al.* 2002; Heinz *et al.* 2002)), nor is there evidence of hot, shock-heated shell that would be present if the radio lobes were expanding supersonically (Kraft *et al.* 2003). It is not clear whether any of these features would be expected in the case of a relic radio source, however. A sensitive low-frequency radio map would give us a better understanding of the possible interaction between radio-emitting plasma and the hot gas.

Second, it is possible that the NGC 7618 gas is oscillating, or 'sloshing', in the gravitational potential because of a recent merger/interaction with a lower mass sub-group. A dust lane has been detected in the optical host galaxy, perhaps indicative of a recent merger

and adding support to this hypothesis (Colbert, Mulchaey, and Zabludoff 2001). Similar structures (on larger scales) to those presented here have been seen in X-ray observations of clusters of galaxies (Markevitch, Vikhlinin, & Mazzotta 2001; Tittley & Henriksen 2005). In this scenario, the gas is oscillating, or 'sloshing', in the dark matter potential due to a recent merger with a sub-cluster. The infall of the sub-cluster drives a shock into the gas that displaces it from the gravitating matter. The gas oscillates around the center of mass, eventually returning to hydrostatic equilibrium via viscous dissipation. Such processes can contribute a significant amount of energy to the gas and may disrupt or prevent the formation of cooling flows in clusters of galaxies. If we naively assume the gas on both sides of the discontinuity is in hydrostatic equilibrium, we find an unphysical discontinuity in the gravitating mass. The apparent mass discontinuity is the result of the non-zero acceleration of the gas inside the discontinuity. The distribution of the gas will reflect the reduced gravity. That is, the acceleration term in Euler's equation is non-zero for gas inside the discontinuity. Assuming that the core is at maximum displacement from the center, the gravitational potential energy of the gas is $U \sim G\Delta M r^{-1} \sim 7 \times 10^{14}$ ergs gm$^{-1}$, or roughly one third of the thermal energy of the gas.

There is one important difficulty with this interpretation, however. On tens of kpc scales, the emission peak of the gas and the optical galaxy (NGC 7618) are both offset (to the N) relative to the larger scale X-ray isophotes (shown green in Figure 2). If the sloshing scenario is correct only the gas and not the galaxy/gravitating mass, should be moving relative to the large scale dark matter halo. The host galaxy should be resting at the center of the gas distribution. In addition, the peak of the X-ray emission lies to the East of the nucleus of the host galaxy, but the larger scale 'sloshing' is North/South. This suggests that there are significant gas motions along perpendicular axes, and that the gas is coupled to the gravitating mass (the stars) along the North/South axis, but partially decoupled along the East/West axis. It is difficult to see how there could be the case unless the merger were off-axis. If this is the case, the merging galaxy should be detectable by an optical census.

The third possibility is that the observed structures are the result of a 'near-miss' flyby of the nearby UGC 12491 group. In this scenario, the UGC 12491 group passed by NGC 7618 from the SE toward its current position to the WNW, and the complex X-ray morphology of NGC 7618 is the result of fluid motions in the gas induced by the gravitational and hydrodynamical interaction. The observed X-ray morphology is the result of the NGC 7618 core being displaced relative to the larger scale gravitational potential, and the surface brightness discontinuity represents a discontinuity in the elemental abundance. X-ray observations of groups and clusters show that the elemental abundance is strongly peaked toward the center. The displacement of the core of a group relative to its halo could create the observed structures.

Hydrodynamic simulations of head-on collisions of equal mass clusters show that the close approach of the cores can create strong non-hydrostatic motions in the gas (Roettiger, Loken, & Burns 1997). Elongation of the dark matter potential, and thus the gas distribution, is a natural consequence of these collisions. In these simulations, the gas becomes partially separated from the gravitating matter and is not a good tracer of the dark matter distribution. The separation between UGC 12491 and NGC 7618 was probably (much) smaller in the past in order to create such a large disturbance in the NGC 7618 gas. The simulations of merging clusters show little separation of the gas from the dark matter as the two clusters initially approach each other. It is only as the cores collide/merge and subsequently separate that significant gas velocities develop. If the current positions of the two groups are, in fact, their closest approach so far, non-hydrostatic effects should just be starting to manifest themselves. Therefore, the two groups must have already passed each other at least once.

There are several difficulties with this scenario, however. If the hotter gas seen in the ASCA/GIS spectrum is shock-heated group gas, the measured temperature ratio (0.8 to 2.3 keV) implies an infall/approach velocity of the two groups of $\sim$1170 km s$^{-1}$ (Landau & Lifshitz 1989), much larger than typical peculiar velocities. It would also be difficult to explain the large amount of hot gas ($\sim$10$^{12}$ M$_\odot$) seen in the ASCA/GIS observation in this scenario under the assumption that this component is entirely shock-heated group gas. The total (thermal) energy of the hotter component is only $\sim$1.3$\times$10$^{61}$ ergs, a reasonable value for the collison of two groups (we note that an AGN outburst could easily supply this much energy to the gas as well (McNamara $et$ $al.$ 2004)). If the hot component is, in fact, shock-heated group gas, it is not bound to the group potential and a transient phenomenon, escaping as a wind.

It is likely that these two groups are gravitationally bound. Ignoring angular momentum (which is not believed to be important on large scales (Hoffman 1986)) and dissipative forces, and assuming that the mass of each group is 10$^{13}$ M$_\odot$, the escape velocity of this pair is $\sim$550 km s$^{-1}$. If either of these groups has a velocity relative to the center of mass larger than this value, the pair will be unbound. This is larger than typical peculiar velocities of galaxies/groups, and it is reasonable to conclude that the system is bound. Significant angular momentum will decrease this value, whereas dissipative forces will increase it. The dynamic parameters of this pair are too poorly known to make a definitive statement, however.

The fourth possibility is that NGC 7618 is falling into a larger gravitational potential. In this scenario, either UGC 12491 is at the center of the potential and NGC 7618 is falling into it, or both NGC 7618 and UGC 12491 are falling into a larger scale potential. The existense of the hotter ($\sim$2.3 keV) gas component in the ASCA/GIS observation (Figure 1)

supports this scenario. The X-ray structures seen in the gas around NGC 7618 are then the result of ram-pressure stripping. This is the classic 'cold-front' scenario discussed by Vikhlinin, Markevitch, & Murray (2001). The effects of ram-pressure stripping on the hot gas atmospheres of early-type galaxies falling into clusters have been studied in *Chandra* observations of NGC 4472, NGC 4552 (falling into the Virgo cluster) and NGC 1404 (falling into/toward NGC 1399, the dominant member of the Fornax cluster) (Biller *et al.* 2004; Machacek *et al.* 2005a,b). In these cases, a sharp surface brightness discontinuity in the direction of infall and a diffuse tail in the opposite direction have been observed. The gas around NGC 7618 is being stripped by hotter, lower density gas that presumably resides in the larger/deeper dark matter halo.

If this scenario is correct, either NGC 7618 is falling into UGC 12491 or both groups are merging with/falling into a larger dark matter potential in which there is no central dominant elliptical galaxy. The high temperature of the second spectral component in the ASCA analysis and the lack of an azimuthally symmetric X-ray halo around UGC 12491 (Figure 1) support the latter hypothesis. This phenomenon has in fact already been observed on a smaller scale in the Pegasus I group (Kraft *et al.* 2005). Neither of the massive ellipticals in this group, NGC 7619 or NGC 7626, lie at the center of the extended X-ray halo. *Chandra* observations of NGC 7619 show a sharp surface brightness discontinuity to the NE (presumably the direction of infall), and an extended, ram-pressure stripped tail in the opposite direction.

If we assume the hotter (2.3 keV) component is in hydrostatic equilibrium with the dark matter potential and that the gas density follows a beta-model profile with $\beta$=0.67 and $r_0$=50 kpc (typical for clusters of galaxies), the gravitating mass, $M_{grav}$, within a radius of 325 kpc of the midpoint between NGC 7618 and UGC 12491 is $\sim$5.6$\times10^{14}$ M$_\odot$. The gas mass, $M_{gas}$, required to account for the observed ASCA/GIS flux of the hotter component within this radius is $\sim$7$\times10^{11}$ M$_\odot$ for this density profile. Ignoring the stellar component, which is insignificant on these spatial scales, the baryon fraction, $f = M_{gas}/M_{grav}$ is $\sim$1.5%. Such a low value of baryon fraction is not improbable for a 2.3 keV cluster. We speculate that this larger dark matter halo may be a 'failed' cluster in which much of the gas was blown off during a cataclysmic event early in its formation (either a merger or a powerful AGN remnant). We caution, however, that the spatial resolution of the ASCA/GIS is poor and our knowledge about the morphology of the gas limited. In addition, this gas may not be in hydrostatic equilibrium, so the uncertainties on both (gas and gravitating) mass estimates are large. A moderate XMM-Newton observation of this pair could measure the temperature and morphology of the hotter component and resolve this issue.

We note that in this scenario the surface brightness discontinuity north of the NGC

7618 nucleus cannot be the stagnation point between the hot gas in NGC 7618 and the gas of this putative larger scale halo. If the observed X-ray surface brightness discontinuity is in fact the stagnation point between these two gases, the temperature of the gas exterior to the discontinuity must be on the order or higher than that of the halo gas (from Bernoulli's equation). The stagnation point therefore must lie beyond the observable emission, and the surface brightness discontinuity represents a contact discontinuity between two fluids. Unless the infall is highly supersonic, the gas interior to the stagnation point should not be highly disturbed and should remain in rough hydrostatic equilibrium in the gravitational potential of NGC 7618. A deeper *Chandra* observation of the central regions of NGC 7618 is required to elucidate the hydrodynamics of the gas.

## 5. Conclusions

We have observed a sharp surface brightness discontinuity in the X-ray emission from the hot gas in the NGC 7618 group, and an X-ray 'tail' extending 70 kpc in the opposite direction in an 8 ks *Chandra*/ACIS-S observation. Archival ASCA/GIS observations indicate the presence of a hotter (2.3 keV) component, although the morphology of this gas is poorly constrained. We conclude that there are three possible explanations for these features. First, the NGC 7618/UGC 12491 pair underwent a recent 'near-miss' flyby. If this is the case, this pair is the nearest early-stage merger of two roughly equal mass groups. Second, UGC 12491 may be at the center of a cluster, and NGC 7618 is falling into it. Third, NGC 7618 and UGC 12491 are both falling into a gas poor cluster with no dominant central elliptical galaxy. Whether the observed features are the result of a group-group merger, or the infall of two groups into a larger dark matter potential, the NGC 7618/UGC 12491 pair is one of the best examples of an ongoing merger in the local Universe. Deeper X-ray observations are required to better constrain the thermodynamic parameters of the gas in the central regions and the larger scale halo. Radio observations will be critical in assessing the role of radio plasma/IGM interactions. If the observed X-ray features are the result of ram-pressure stripping or a merger interaction between the groups, the effects on the relic radio halo are likely to have been dramatic. A detailed optical census including velocities of the other galaxies in the both groups will be useful to constrain their dynamics and their relationship to the larger dark matter potential.

## REFERENCES

Biller, B. A., Jones, C., Forman, W. R., Kraft, R., Enßlin, T. 2004, ApJ, **613**, 238.

Briel, U. G., Finoguenov, A., and Henry, J. P. 2004, A.& A., **426**, 1.

Canosa, C. M., Worrall, D. M., Hardcastle, M. J., and Birkinshaw, M. 1999, MNRAS, **310**, 30.

Colbert, J. W., Mulchaey, J. S. & Zabludoff, A. I. 2001, AJ, **121**, 808.

Ebeling, H., Mullis, C. R., & Tully, R. B. 2002, ApJ, **580**, 774.

Ficarra, A., Grueff, G., & Tomassetti, G. 1985, A.& A.S., **59**, 255.

Hales, S. E. G., Baldwin, J. E., Warner, P. J. 1993, MNRAS, **263**, 25.

Heinz, S., Choi, Y.-Y., Reynolds, C. S., & Begelman, M. C. 2002, ApJ, **569**, 79.

Henry, J. P., Finoguenov, A., and Briel, U. G. 2004, ApJ, **615**, 181.

Hoffman, Y. 1986, ApJ, **301**, 65.

Jones, C. & Forman, W. 1984, ApJ, **276**, 38.

Jones, C. & Forman, W. 1984, ApJ, **511**, 65.

Jones, C., Forman, W., Vikhlinin, A., Markevitch, M., David, L., Warmflash, A., Murray, S., & Nulsen, P. E. J. 2002, ApJ, **567**, L115.

Jones, C., *et al.* 2005, submitted.

Kim, D.-W. & Fabbiano, G. 1995, ApJ, **441**, 182.

Kraft, R. P., *et al.* 2003, ApJ, **601**, 221.

Kraft, R. P. *et al.* 2005, in preparation.

Landau, L. D., & Lifshitz, E. M. 1989, 'Fluid Mechanics', 2nd ed., Butterworth and Heineman.

Machacek, M., Dosaj, A., Forman, W., Jones, C., Markevitch, M., Vikhlinin, A., Warmflash, A., Kraft, R. 2005, ApJ, **621**, 663.

Machacek, M., *et al.* 2005, submitted.

Markevitch, M., *et al.* 2000, ApJ, **541**, 542.

Markevitch, M., Vikhlinin, A., and Mazzotta, P. 2001, ApJ, **562**, L153.

Mazzotta, P., Markevitch, M., Vikhlinin, A., Forman, W. R., David, L. P., & VanSpeybroeck, L. 2001, ApJ, **555**, 205.

McNamara, B., *et al.* 2000, ApJ, **534**, L135.

McNamara, B., *et al.* 2004, Nature, **433**, 45.

Mohr, J. J., Evrard, A. E., Fabricant, D. G., Geller, M. J. 1995, ApJ, **447**, 8.

Nulsen, P. E. J., David, L. P., McNamara, B. R., Jones, C., Forman, W. R., Wise, M. 2002, ApJ, **568**, 163.

Roettiger, K., Loken, C., and Burns, J. O. 1997, ApJS, **109**, 307.

Spergel, D., *et al.* 2003, ApJS, **148**, 175.

Tittley, E. R. & Henriksen, M. 2005, ApJ, **618**, 227.

Vikhlinin, A., McNamara, B. R., Hornstrup, A., Quintana, H., Forman, W., Jones, C., Way, M. 1999, ApJ, **520**, L1.

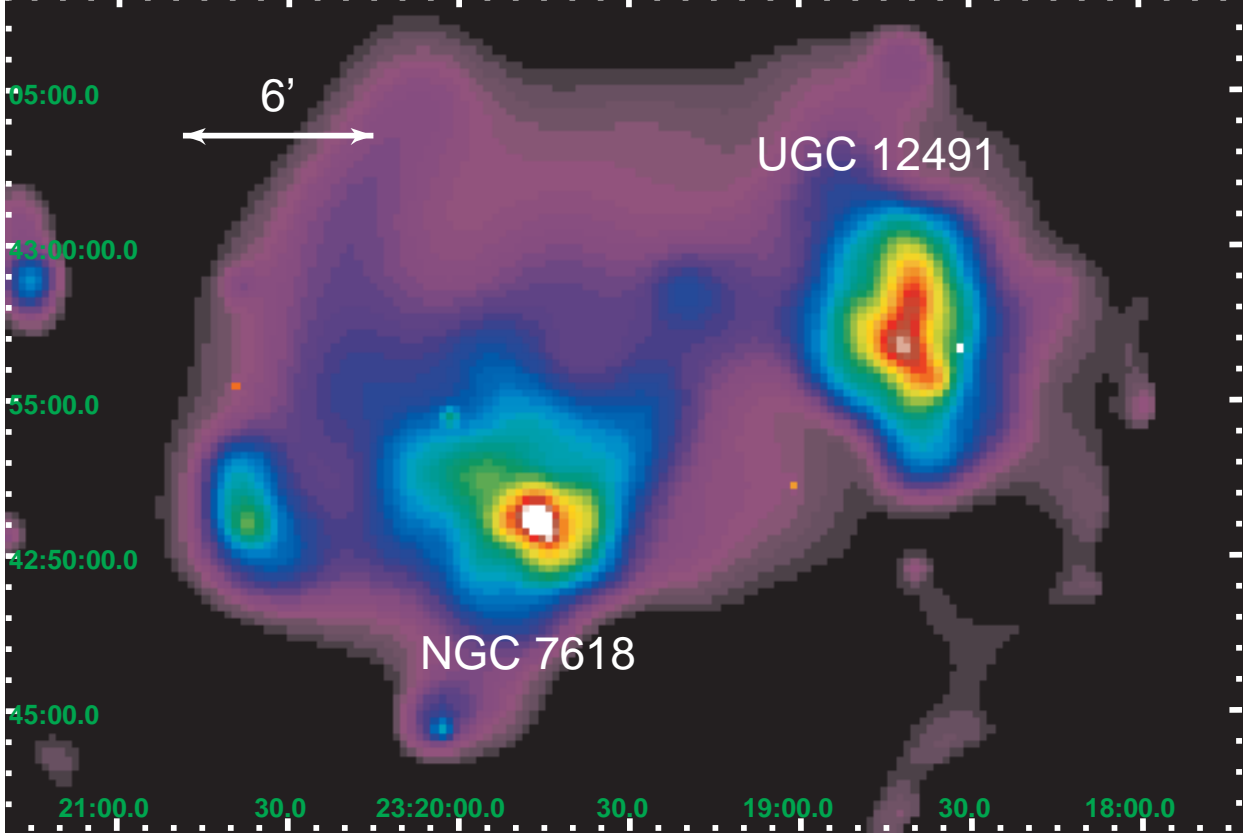Vikhlinin, A., Markevitch, M., & Murray, S. S. 2001, ApJ, **551**, 160.

Fig. 1.— Adaptively smoothed ASCA/GIS image of NGC 7618 and UGC 12491. The minimum (violet) and maximum (white) surface brightnesses in this image are ∼38.4 and 134.2 cts arcmin$^{-2}$, respectively. The background, estimated from an off-source region at the edge of the field of view is 23.5±1.1 cts arcmin$^{-2}$. The violet regions in this image are therefore significant at more than 10$\sigma$.
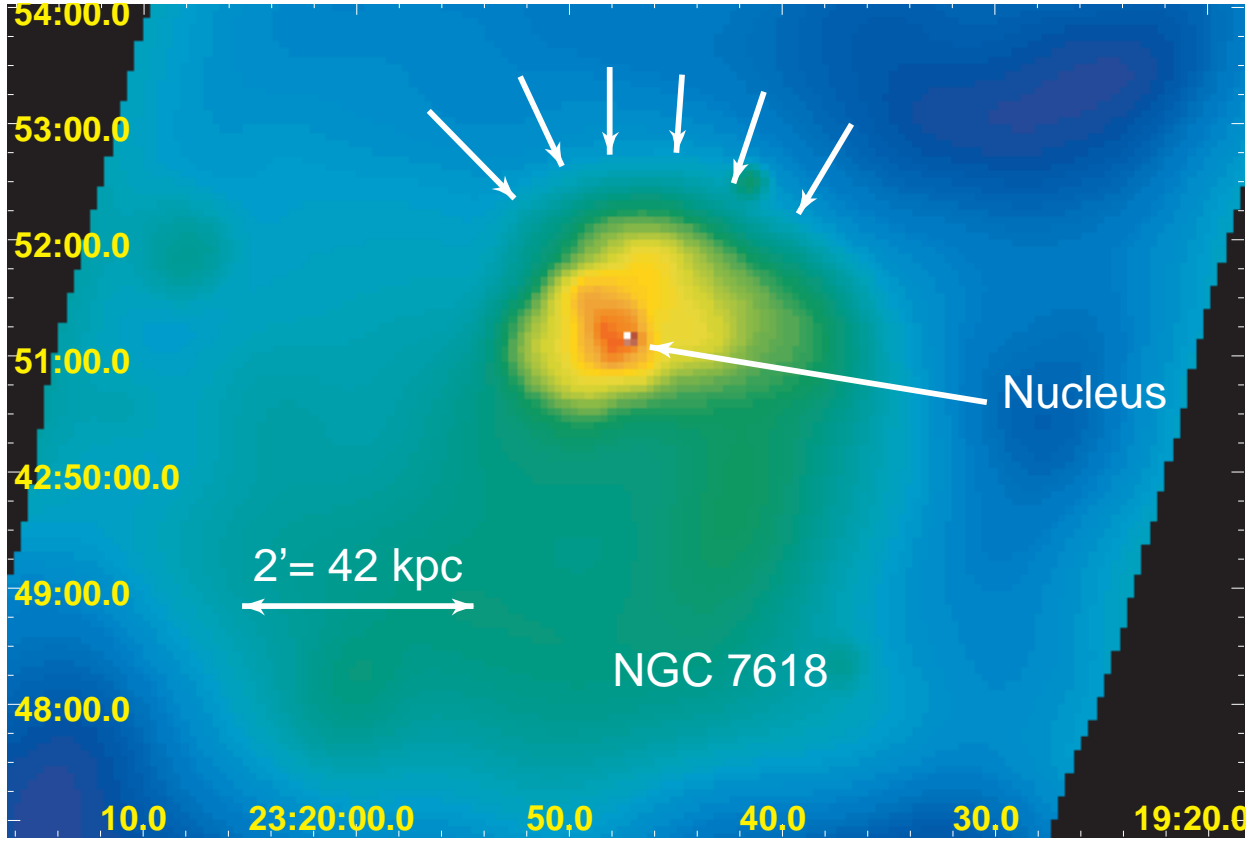
Fig. 2.— Adaptively smoothed, exposure corrected, background subtracted Chandra/ACIS-S image of NGC 7618 in the 0.5-2.0 keV band. The white arrows denote the surface brightness discontinuity.
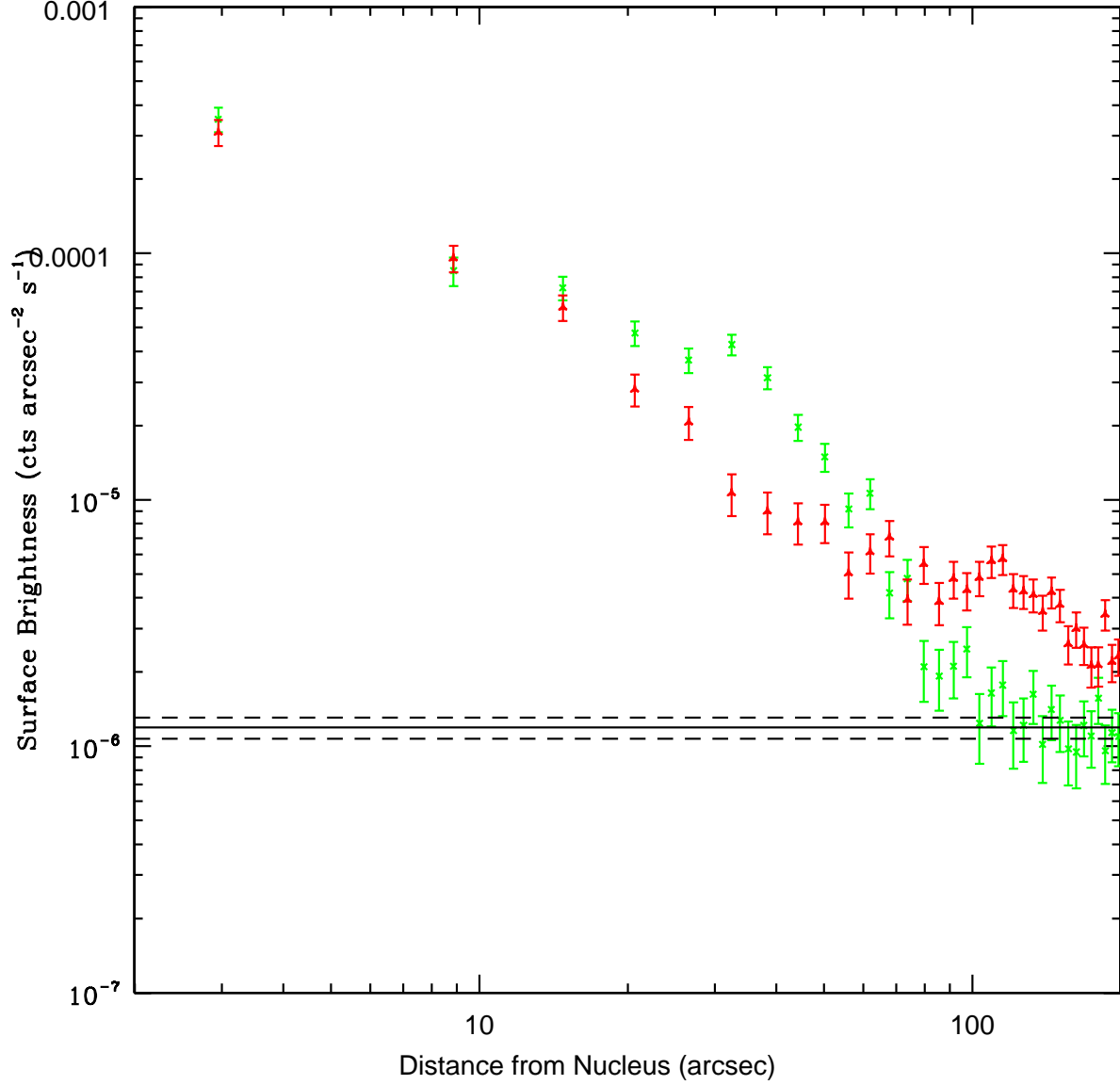
Fig. 3.— Surface brightness profiles in 90° sectors to the North (green) and South (red) centered on the nucleus of NGC 7618. The solid and dashed lines indicate the background level and uncertainty, respectively, estimated from a distance region of the S3 chip. Note the excess of counts in the Southern 'tail' from 70″ to 200″.
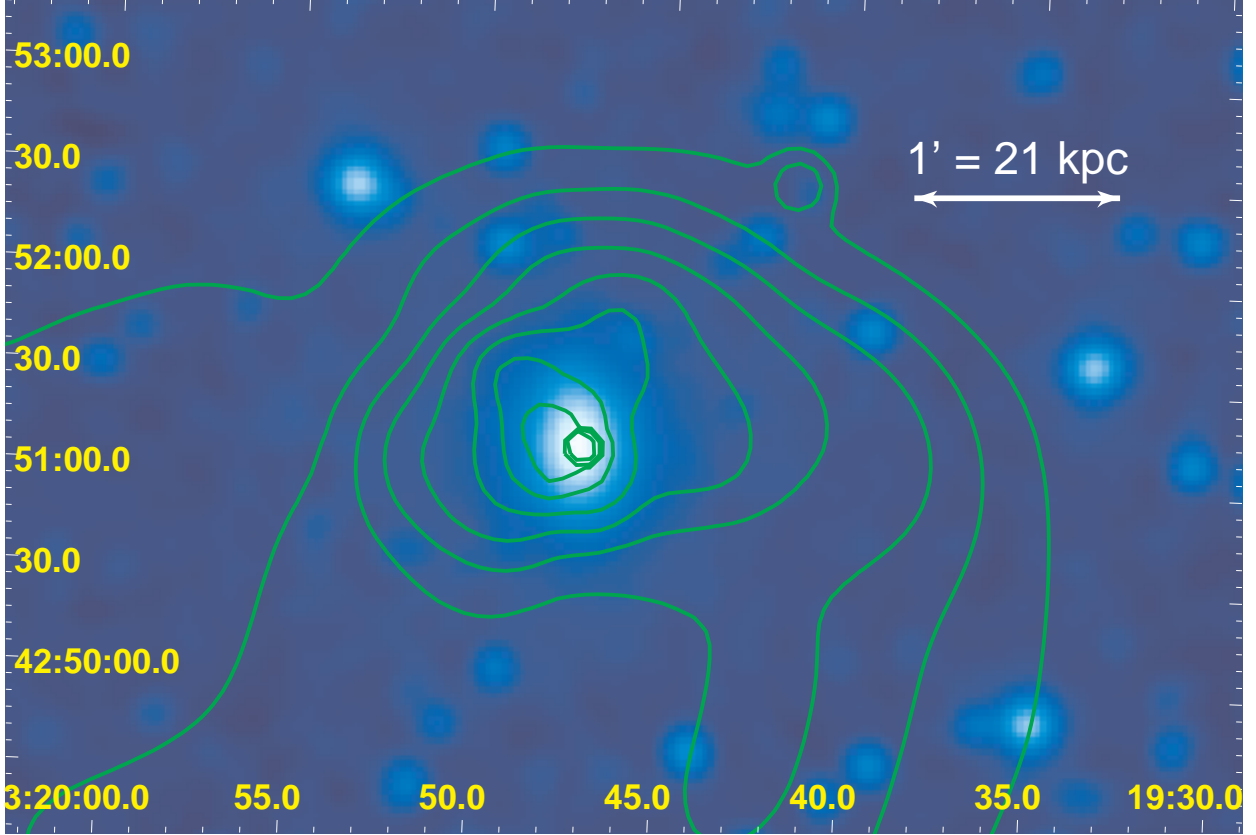
Fig. 4.— Contours from previous image overlaid onto optical/DSS image of NGC 7618. The active nucleus is co-incident with the peak of the optical isophotes. The contours correspond to a surface brightness of 3, 5, 9, 16, 28, 50, 88, 155, 274, and 484 $\times10^{-5}$ cts arcsec$^{-2}$ s$-1$.
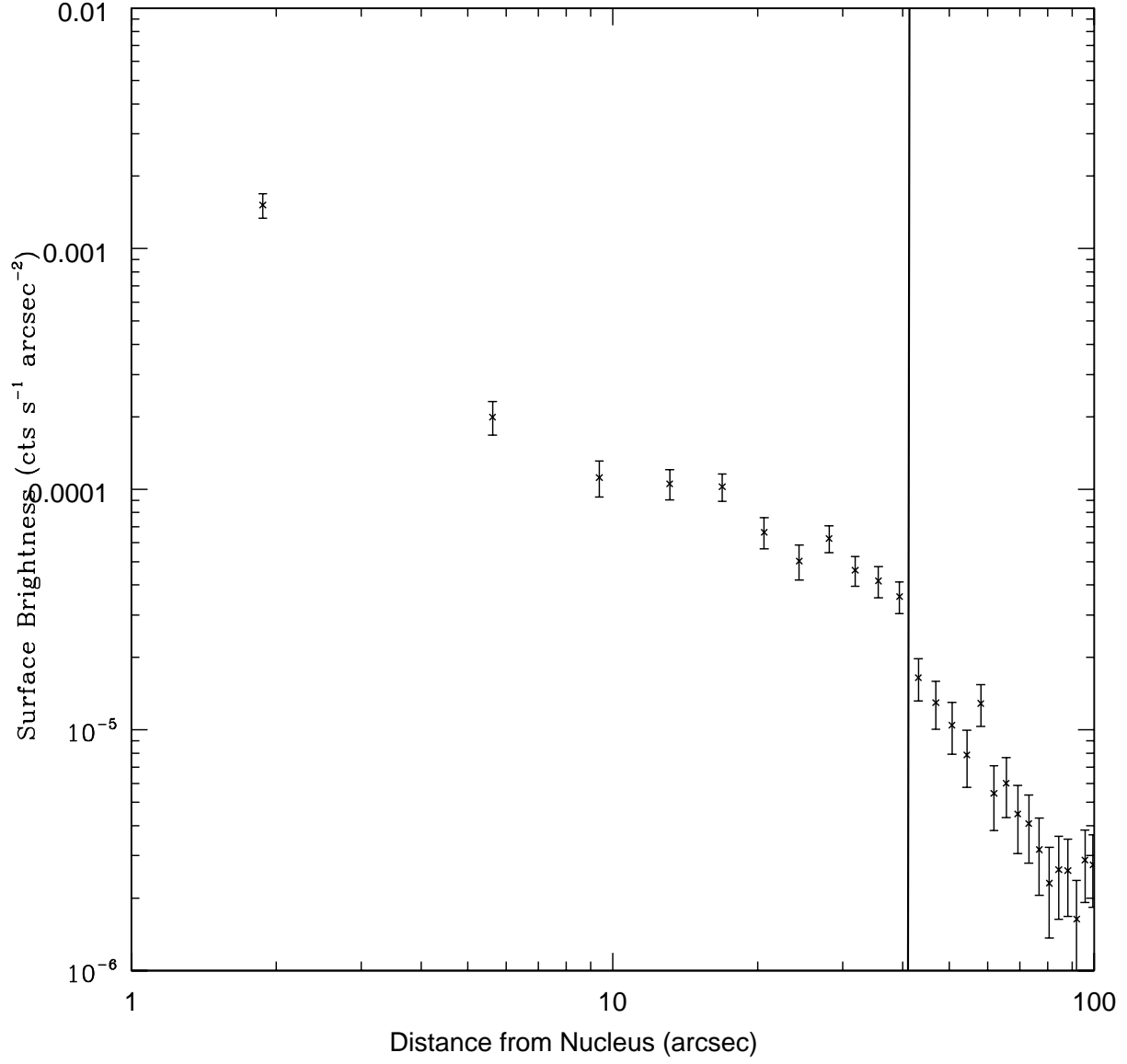
Fig. 5.— Surface brightness profile in a 60° sector N of the nucleus across the discontinuity. The position of the surface brightness discontinuity is denoted by the dark vertical line.
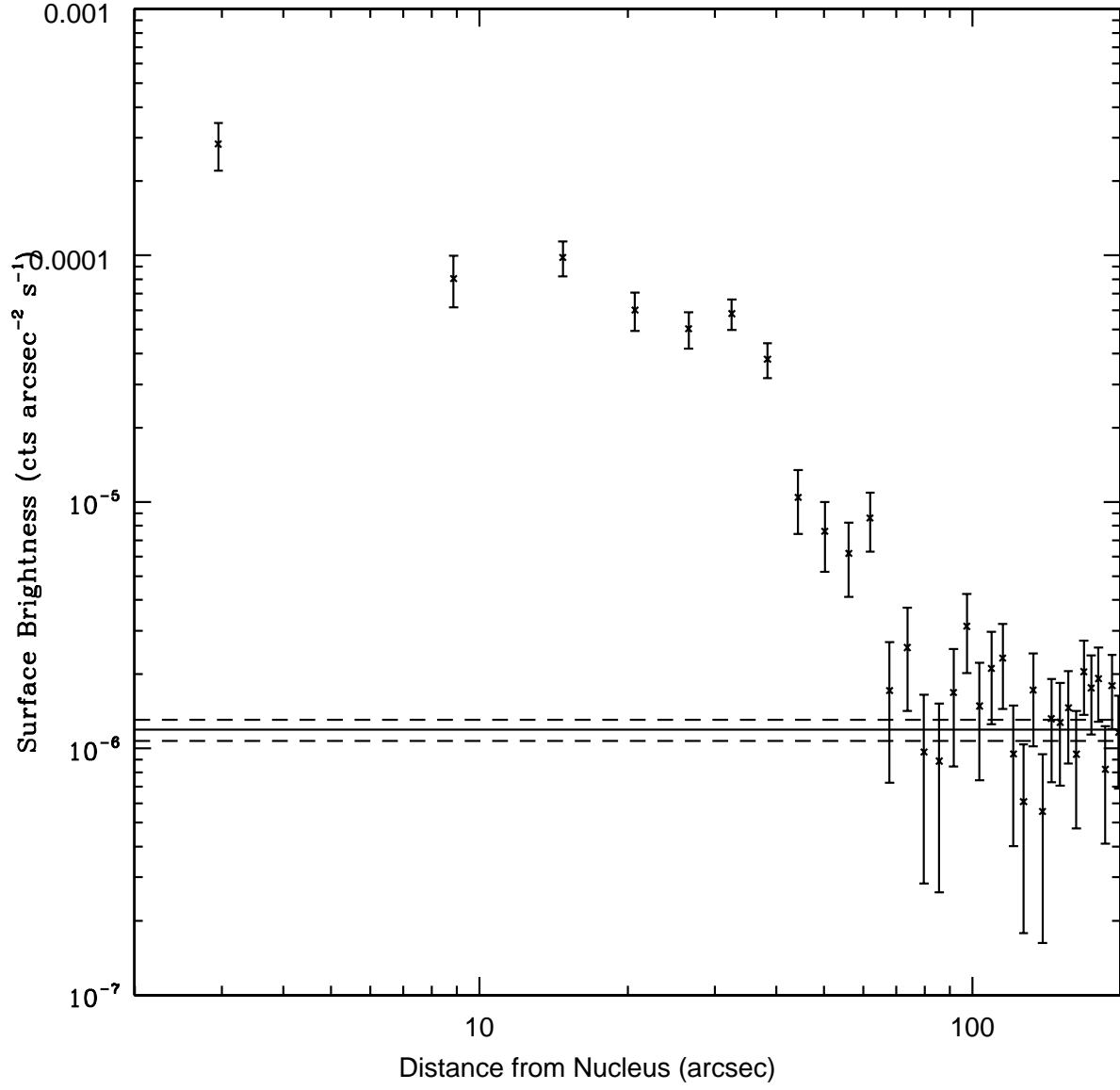
Fig. 6.— Surface brightness profile in a 30° sector to the NE of the nucleus across the discontinuity. The position of the surface brightness discontinuity is denoted by the dark vertical line.

|  | NGC 7618 | UGC 12491 |
|---|---|---|
| $m_B$ | 14.0 | 14.9 |
| $M_B$ | -21.3 | -20.2 |
| $z$ | 0.017309 | 0.017365 |
| Distance (Mpc) | 74.1 | 74.3 |
| $L_X$ (ergs s$^{-1}$) | $6.9{\times}10^{42}$ | $6.2{\times}10^{42}$ |
| X-ray Radius | $\sim$170 kpc | $\sim$200 kpc |

Table 1: Summary of the X-ray and optical properties of the NGC 7618 and UGC 12491 galaxies. The X-ray luminosity is in the 0.1-10 keV bandpass (unabsorbed) within 7′ (146 kpc) of the nucleus. Absolute magnitudes have been corrected for extinction.

| | NGC 7618 | UGC 12491 | Diffuse |
|---|---|---|---|
| Single Temperature Fits | | | |
| $k_BT$ (keV) | $1.43^{+0.08}_{-0.14}$ | $1.32^{+0.10}_{-0.13}$ | $2.32^{+0.50}_{-0.34}$ |
| Flux | $3.06 \times 10^{-12}$ | $5.37 \times 10^{-12}$ | $2.53 \times 10^{-12}$ |
| $\chi^2_\nu$ | 1.95 | 1.60 | 0.73 |
| Two Temperature Fits | | | |
| $k_BT_1$ (keV) | 0.80 | $0.86^{+0.16}_{-0.09}$ | |
| Flux | $2.26 \times 10^{-12}$ | $3.69 \times 10^{-12}$ | |
| $k_BT_2$ (keV) | $2.21^{+0.33}_{-0.67}$ | $2.26^{+1.19}_{-0.35}$ | |
| Flux | $1.48 \times 10^{-12}$ | $2.15 \times 10^{-12}$ | |
| $\chi^2_\nu$ | 1.03 | 0.78 | |

Table 2: Best-Fit Temperatures and Fluxes of the ASCA/GIS data in three regions. All uncertainties are 90% confidence for one parameter of interest. Units of fluxes are ergs cm$^{-2}$ s$^{-1}$ (unabsorbed) in the 0.5-2.0 keV band.